Computer-Aided Noise Analysis of MESFET and HEMT Mixers

VITTORIO RIZZOLI, MEMBER, IEEE, FRANCO MASTRI, AND CLAUDIO CECCHETTI

Abstract—**The paper discusses a novel numerical approach to the noise analysis of MESFET and HEMT mixers of arbitrary topology. A qualitative picture of the complex physical mechanisms responsible for the generation of the IF noise is first outlined, and the corresponding computational algorithms are presented. The derivation of a noisy nonlinear model for the microwave FET is then addressed, and it is shown that a satisfactory solution to this apparently formidable problem can be obtained by combining a conventional time-domain model with standard noise information. The method has been implemented in a computer program designed to work in conjunction with an existing general-purpose harmonic-balance simulator. An example of application is described in detail to demonstrate the excellent performance of this new software tool.**

I. Introduction

NONLINEAR CAD techniques for microwave mixer analysis and optimization are well established. Conversion-matrix methods have been in use for years [1]–[5], and full nonlinear approaches based on the harmonic-balance concept have recently become available as standard capabilities of commercial general-purpose simulators (e.g., [6] and [7]). An important shortcoming of existing software, however, is that mixer noise analysis is not addressed in a systematic way.

As a matter of fact, even from a theoretical viewpoint, there is a considerable lack of information concerning the noise analysis problem for FET mixers. While diode mixer noise has been exactly analyzed in the classic papers by Held and Kerr [1] and Kerr [2], an extension to the FET case does not seem to be available. A few partial solutions have, indeed, been proposed. For instance, Tie and Aitchison [8] introduce an approximate explicit formula for the gate mixer, while Dreifuss *et al.* [9] make use of a phenomenological expression of the noise correlation matrix. However, these attempts have so far not led to a generally accepted computational procedure, as witnessed by recent books on the subject [10], [11]. More recently, a generalized computational scheme for noise calculation in nonlinear circuits has been introduced [12]. In this paper we show that the concepts discussed in [12] can be developed into a software tool suitable for use in microwave engineering practices. This software is designed to work in conjunction with an existing general-purpose nonlinear simulator based on the harmonic-balance technique [13]. The compatibility is ensured by the fact that all noise calculations are carried out in the frequency domain.

The applications described in the paper mainly concern MESFET mixers. However, it is generally acknowledged that the same nonlinear equivalent circuits usable for MESFET's are equally valid for HEMT's (e.g., [14]) and that the basic noise equations are also similar for the two kinds of devices [15]. Thus the noise analysis programs described here are directly applicable to HEMT mixers. The analysis of DGFET mixers is also possible, provided that an equivalent representation of the dual-gate FET as the cascode connection of two conventional FET's is available. The general-purpose numerical approach adopted is warranted by the wide variety of mixer topologies, both single- and multiple-device, that are of interest for microwave applications (e.g., [10], [16], and [17]).

II. Noise Analysis

The goal of the noise analysis is to find the spectral distribution of the noise power actually delivered to the IF load. From this information the mixer noise figure or any other quantity of interest can be derived in a straightforward way. For instance, let us denote by $dN(\omega)$ the average power delivered by the spectral components of the load noise waveforms lying between ω and $\omega + d\omega$ when the load itself is assumed to be noiseless, and the source is kept at the reference temperature $T_0 = 290$ K. Then the SSB spot noise figure at a given ω_{IF} may be expressed as

$$F(\omega_{IF}) = \frac{2\pi dN(\omega_{IF})}{K_B T_0 G(\omega_{RF})\, d\omega} \tag{1}$$

where K_B is Boltzmann's constant, and G is the transducer conversion gain between the radio frequency ω_{RF} and the IF of interest.

In order to compute $dN(\omega)$ we must perform three fundamental steps. We first need a comprehensive qualitative picture of the complex nonlinear phenomena that take

Manuscript received November 16, 1988; revised April 3, 1989. This work was supported by the Italian Ministry of Education and by the Istituto Superiore delle Poste e delle Telecomunicazioni (ISPT). Part of this paper was the subject of an invited presentation at the Workshop on Non Linear CAD Tools for Microwave and Millimetre-Wave (Integrated) Circuit Analysis, held in conjunction with the 18th European Microwave Conference, Stockholm, Sweden, 1988.

V. Rizzoli is with the Dipartimento di Elettronica, Informatica e Sistemistica, University of Bologna, Bologna, Italy

F. Mastri is with the Fondazione Guglielmo Marconi, Bologna, Italy.

C. Cecchetti is with the Fondazione Ugo Bordoni, Villa Griffone, 40044 Pontecchio Marconi, Bologna, Italy.

IEEE Log Number 8928990.

0018-9480/89/0900-1401$01.00 ©1989 IEEE

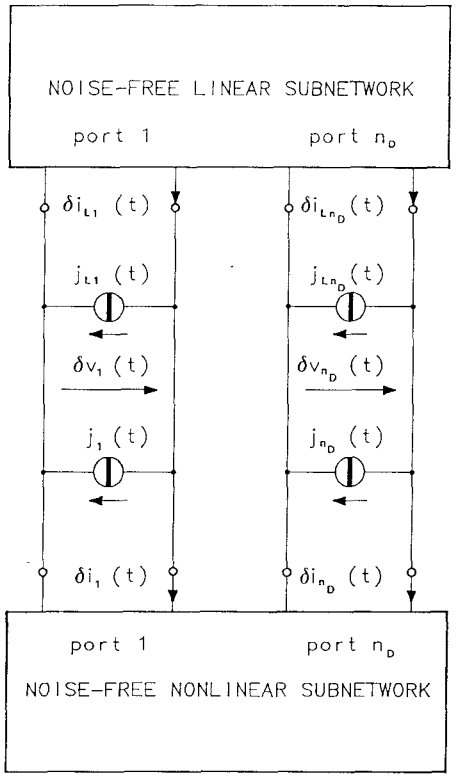

Fig 1. General equivalent representation of a noisy mixer. The $j_L(t)$ are Norton equivalent noise current sources at the linear subnetwork ports. The $j(t)$ are noise current sources at the intrinsic FET gate and drain terminals.

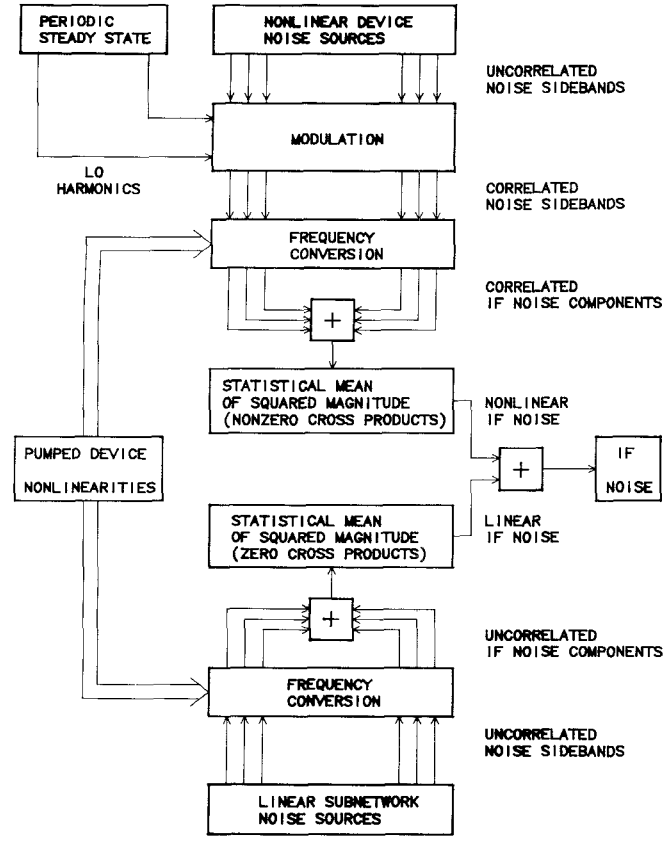

Fig 2. Flowchart of the IF noise generation mechanism.

place in the circuit to provide a suitable basis of understanding for the subsequent mathematical developments. Then we have to carry out a perturbational analysis of the LO-pumped steady state, which will enable us to compute the power transferred to the load from any source injecting into the circuit a small signal in the presence of the local oscillator regime. Finally, we have to derive the necessary information on the statistical properties of the noise sources, starting from the available information on the passive subnetwork and on the active device.

From a practical viewpoint, our purpose is to develop an analysis program to be run in conjunction with a general-purpose harmonic-balance (HB) simulator [13]. We shall thus refer to the equivalent representation of the mixer shown in Fig. 1, which may be considered an extension of the usual decomposition adopted to apply the piecewise HB technique [18]. For our present purposes the nonlinear subnetwork is just a collection of intrinsic FET (or HEMT) chips, while all (linear) parasitic elements are included in the linear part.

From the viewpoint of noise analysis, the circuit in Fig. 1 is a sort of Norton equivalent. Of course, it is exactly a Norton equivalent for the linear subnetwork, while for the FET chips it is simply obtained from the usual transistor representation consisting of a noiseless intrinsic device with a noise current source connected across the gate–source port and one across the drain–source port (e.g., [19]). All noise current sources are explicitly shown in the equivalent circuit.

From the viewpoint of nonlinear analysis, the circuit in Fig. 1 is a perturbational scheme. We take for granted the existence of a stable time-periodic local oscillator regime and analyze the effects of superimposing the noise sources on such periodic steady state under the assumption that the noise spectral components are small compared to the local oscillator harmonics.

Fig. 2 is a pictorial representation of the physical mechanism giving rise to the IF noise. Since a dominant steady-state regime exists in the circuit, every aspect of its electrical behavior is scanned in a time-periodic fashion at a rate corresponding to the local oscillator period. In the frequency domain, this implies the interaction of all spectral components whose frequencies differ by integral multiples of the local oscillator frequency. For a spot noise calculation at a given IF, we thus have to consider all noise sidebands whose frequencies differ from the selected IF by such amounts. This means that a generic noise waveform will be represented by

$$n(t) = \sum_k N_k \exp\left[j(\omega_{IF} + k\omega_0)t\right] \qquad (2)$$

where ω_0 is the LO angular frequency and N_k is the random complex amplitude of the pseudosinusoidal noise component at the kth sideband, $\omega_{IF} + k\omega_0$. From a physical viewpoint, (2) represents that component of the actual

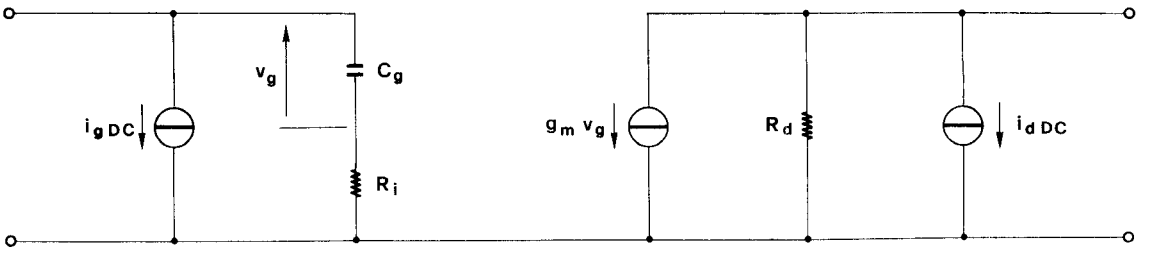

Fig. 3. Equivalent circuit of a noisy intrinsic FET.

noise waveform whose spectrum lies in a small neighborhood $d\omega$ of ω_{IF}.

The qualitative noise picture obtained from Fig. 2 is now as follows. There are two kinds of noise sources acting in the circuit: the nonlinear device sources and the linear subnetwork sources. If the nonlinear devices were at rest, that is, only dc biased, the nonlinear noise source sidebands would not be correlated and would depend on the device bias points. Such sources are thus modulated by the local oscillator waveforms. The actual nonlinear noise sidebands are then partly correlated, because each one is a combination of the original uncorrelated dc sidebands. Because of the frequency conversion in the pumped nonlinear device, each noise sideband generates an IF noise component, and such components are correlated. To find the IF noise power generated by the nonlinear device sources we have to take the squared magnitude of the sum of all such components and then compute its statistical mean by taking the correlation coefficients into account.

Of course, the situation is much simpler for the linear-subnetwork noise sources. These generators are not affected by the local oscillator regime, since their statistical properties depend only on the linear subnetwork topology and temperature. Their uncorrelated noise sidebands are converted by the pumped nonlinear device, resulting in uncorrelated IF noise contributions which may be superimposed in power. The same is true for the linear and nonlinear IF noise contributions, which are clearly uncorrelated due to their independent physical origins.

Note that from the above picture the frequency conversion produced by the FET nonlinearities clearly appears to be the heart of the IF noise generation mechanism.

Still following Fig. 2, we now outline the steps of the noise-analysis algorithm. We start from a general time-domain description of the active devices in the parametric form

$$\begin{aligned} \boldsymbol{v}(t) &= \boldsymbol{u}\left[\boldsymbol{x}(t), \frac{d\boldsymbol{x}}{dt}, \cdots, \frac{d^n\boldsymbol{x}}{dt^n}\right] \\ \boldsymbol{i}(t) &= \boldsymbol{w}\left[\boldsymbol{x}(t), \frac{d\boldsymbol{x}}{dt}, \cdots, \frac{d^n\boldsymbol{x}}{dt^n}\right] \end{aligned} \tag{3}$$

where $\boldsymbol{v}$ and $\boldsymbol{i}$ are vectors of voltages and currents at the device ports, $\boldsymbol{u}$ and $\boldsymbol{w}$ are vector-valued nonlinear functions, and $\boldsymbol{x}$ is a vector of time-dependent quantities used as state variables. This approach is illustrated in detail in [13]. All vectors in (3) have the same size n_D, equal to the overall number of device ports. Equations (3) are very convenient for a FET when the voltage across the gate-to-source capacitance is chosen as a state variable (see Fig. 3). When using the piecewise harmonic-balance (PHB) technique for nonlinear circuit analysis, the network is described in terms of a state vector $\boldsymbol{X}$ of all state-variable harmonics. Likewise, the set $\boldsymbol{X}_0$ of the dc components of $\boldsymbol{x}(t)$ identifies the active-device bias point.

Referring to Fig. 1, let us denote by $\boldsymbol{j}_{dc}(t, \boldsymbol{X}_0)$ the noise sources introduced by the nonlinear components ("nonlinear" noise sources) when the local oscillator pump is suppressed and the active devices are dc biased at the point $\boldsymbol{X}_0$ ("static" condition). These static noise sources are random functions of time, but are deterministic functions of $\boldsymbol{X}_0$. Under dynamic conditions, i.e., when the LO drive is applied, the nonlinear noise sources are thus modulated in a deterministic way by the time-periodic LO regime. We write the relationship between static and dynamic nonlinear noise sources in the form

$$\boldsymbol{j}(t) = \boldsymbol{h}(t)\boldsymbol{j}_{dc}(t, \boldsymbol{X}_0) \tag{4}$$

where $\boldsymbol{h}(t)$ is a diagonal matrix of size n_D and is time periodic with period $2\pi/\omega_0$. Each entry of $\boldsymbol{h}(t)$ plays the role of a modulation law for the corresponding static noise source. The Fourier expansion of $\boldsymbol{h}(t)$ may be written

$$\boldsymbol{h}(t) = \sum_p \boldsymbol{H}_p \exp(jp\omega_0 t) \tag{5}$$

where $\boldsymbol{H}_p$ is a diagonal matrix of size n_D, and $\boldsymbol{H}_{-p} = \boldsymbol{H}_p^*$ (* = transposed conjugate). The details of the derivation of $\boldsymbol{h}(t)$ for a FET will be given in Section III.

Making use of expressions similar to (2) for the nonlinear noise sources, from (4) and (5) we get

$$\boldsymbol{J}_p = \sum_s \boldsymbol{H}_{p-s}\boldsymbol{J}_{dcs}. \tag{6}$$

Equation (6) shows that the dynamic noise sidebands are partly correlated even though the static ones are not. Finally, if we introduce the correlation matrix of the static nonlinear noise sources, namely $\boldsymbol{C}_{dc}(\omega)$, from (6) the correlation matrix of the dynamic sources is easily derived:

$$\langle \boldsymbol{J}_p \boldsymbol{J}_q^* \rangle = \sum_s \boldsymbol{H}_{p-s}\boldsymbol{C}_{dc}(\omega_{IF} + s\omega_0)\boldsymbol{H}_{s-q} \tag{7}$$

where $\langle\ \rangle$ indicates the statistical mean. Note that $\boldsymbol{C}_{dc}(\omega)$ is a block diagonal of the individual device correlation matrices (each 2×2 in size), which may be regarded as known for FET (or HEMT) devices (see Section III).

For the linear subnetwork, the correlation matrix $\boldsymbol{C}_L(\omega)$ of the equivalent noise current sources shown in Fig. 1 is defined by

$$\langle \boldsymbol{J}_{Lp} \boldsymbol{J}_{Lq}^* \rangle = \delta_p^q \boldsymbol{C}_L(\omega_{\mathrm{IF}} + p\omega_0) \tag{8}$$

where δ is Kronecker's symbol. Note that in the derivation of $\boldsymbol{C}_L$ the IF load resistor must be treated as a noise-free component for the definition (1) of noise figure to apply. An important point is that general algorithms allowing this to be done for a completely arbitrary linear subnetwork topology are available in the technical literature (e.g., [20]).

When the noise-source currents (Fig. 1) are superimposed on the local oscillator regime, the steady state is perturbed in the sense that relatively small random disturbances are added to the steady-state waveform of each time-dependent quantity. For a spot noise calculation at a given ω_{IF}, the perturbations have the form (2) and can thus be represented in the frequency domain by the vectors of all sideband phasors. The perturbations of the state variables, the voltages, and the currents at the device ports will be represented by the vectors $\delta \boldsymbol{X}, \delta \boldsymbol{V}, \delta \boldsymbol{I}$, respectively. Similarly, for the linear and nonlinear noise currents we introduce the vectors $\boldsymbol{J}_L$ and $\boldsymbol{J}$ (see Fig. 1).

The noise-sideband phasors are related by the conventional frequency-domain equations of the linear subnetwork and by the conversion equations of the nonlinear devices [21]. For the linear subnetwork we may write (see Fig. 1)

$$\boldsymbol{A}\delta \boldsymbol{V} + \boldsymbol{B}(\delta \boldsymbol{I} + \boldsymbol{J} + \boldsymbol{J}_L) = 0 \tag{9}$$

where $\boldsymbol{A}$ and $\boldsymbol{B}$ are block diagonals of the conventional circuit matrices at all sidebands. For the nonlinear devices we have to carry out a first-order perturbational analysis of the LO regime [12]. This leads from the time-domain nonlinear device equations (3) to a set of frequency-domain linear equations in the sideband phasors (conversion equations) of the form

$$\begin{aligned} \delta \boldsymbol{V} &= \boldsymbol{P}\delta \boldsymbol{X} \\ \delta \boldsymbol{I} &= \boldsymbol{Q}\delta \boldsymbol{X} \end{aligned} \tag{10}$$

where $\boldsymbol{P}$ and $\boldsymbol{Q}$ are conversion matrices.

The conversion matrices may be directly derived from the device equations (3) by the following algorithm [21]. Let us introduce the Jacobian matrices of $\boldsymbol{u}$ and $\boldsymbol{w}$ in (3) with respect to the state vector $\boldsymbol{x}$ and its time derivatives. In steady-state conditions (no perturbations) all such quantities are time periodic with period $2\pi/\omega_0$ and can be represented by Fourier expansions. We write

$$\begin{aligned} \left.\frac{\partial \boldsymbol{u}}{\partial \boldsymbol{y}_m}\right|_{ss} &= \sum_p \boldsymbol{C}_{m,p} \exp(jp\omega_0 t) \\ \left.\frac{\partial \boldsymbol{w}}{\partial \boldsymbol{y}_m}\right|_{ss} &= \sum_p \boldsymbol{D}_{m,p} \exp(jp\omega_0 t), \qquad (m = 0,1,\cdots,n) \end{aligned} \tag{11}$$

where $\boldsymbol{y}_0 = \boldsymbol{x}$ and $\boldsymbol{y}_m = d^m \boldsymbol{x}/dt^m$. We then define the submatrices

$$\begin{aligned} \boldsymbol{P}_{k,p} &= \sum_{m=0}^{n} [j(\omega_{\mathrm{IF}} + k\omega_0)]^m \boldsymbol{C}_{m,p} \\ \boldsymbol{Q}_{k,p} &= \sum_{m=0}^{n} [j(\omega_{\mathrm{IF}} + k\omega_0)]^m \boldsymbol{D}_{m,p}. \end{aligned} \tag{12}$$

Finally, the conversion matrices are given by

$$\boldsymbol{P} \equiv [\boldsymbol{P}_{k,s-k}] \qquad \boldsymbol{Q} \equiv [\boldsymbol{Q}_{k,s-k}] \tag{13}$$

where s is the row index, and k is the column index, of the generic submatrix.

Note that (9) to (13) represent a generalized approach to the conventional conversion-matrix analysis of microwave mixers. Besides being fast and general, this type of approach is also numerically accurate. The availability of general-purpose nonlinear simulators with multitone analysis capabilities [13] allows this accuracy to be quantitatively established; for instance, by the above-described algorithm, all elements of the conversion matrix of a pumped FET can be found with at least five exact decimal digits in both magnitude and phase.

By combining (9) and (10) with conventional linear circuit analysis techniques, the noise-sideband voltage and current phasors at any point within the mixer can easily be expressed as functions of the noise sources. In particular, we are interested in the noise current sidebands $\delta I_{\mathrm{IF}k}$ through the IF load resistor R_{IF}. Since (9) and (10) are linear, $\delta I_{\mathrm{IF}k}$ is a linear combination of the noise-source sideband phasors $\boldsymbol{J}_{Lp}$ and $\boldsymbol{J}_p$, that is,

$$\delta I_{\mathrm{IF}k} = \sum_p \boldsymbol{T}_{kp}(\boldsymbol{J}_{Lp} + \boldsymbol{J}_p) \tag{14}$$

where $\boldsymbol{T}_{kp}$ represents a sideband-to-sideband conversion matrix. A detailed derivation of $\boldsymbol{T}_{kp}$ is reported in [12]. If we now recall that the sideband count is such that $k = 0$ yields the intermediate frequency, from (14), (7), and (8) we obtain the noise power to be used in the noise figure definition (1) as

$$\begin{aligned} dN(\omega_{\mathrm{IF}}) &= R_{\mathrm{IF}} \sum_p \boldsymbol{T}_{0p} \boldsymbol{C}_L(\omega_{\mathrm{IF}} + p\omega_0) \boldsymbol{T}_{0p}^* \\ &+ R_{\mathrm{IF}} \sum_{p,q} \boldsymbol{T}_{0p} \left[\sum_s \boldsymbol{H}_{p-s} \boldsymbol{C}_{\mathrm{dc}}(\omega_{\mathrm{IF}} + s\omega_0) \boldsymbol{H}_{s-q} \right] \boldsymbol{T}_{0q}^*. \end{aligned} \tag{15}$$

Equation (15) may be considered as the quantitative statement of the qualitative noise picture given in Fig. 2. Here mixer noise is essentially described as a frequency-conversion effect, the pattern of interfrequency power flow being determined by the set of sideband-to-sideband conversion matrices.

As a final remark we note that the above analysis apparently does not make any mention of the noise injected into the mixer by the local oscillator. As a matter of fact, this additional problem may be treated in two different ways. One is to consider the combined mixer and local oscillator as a single circuit, and to apply the same analysis

to this extended nonlinear network. On the other hand, if the detailed topology of the local oscillator is not available, its noise can be treated as additive noise due to an additional noise source acting in the circuit. Of course the statistical properties of this source must be known *a priori* for the calculation to be possible. The IF noise generated by this source may then be computed by an equation having the same structure as the second term on the right-hand side of (15), with the quantity enclosed in square brackets replaced by the correlation matrix of the local-oscillator noise sidebands.

III. Nonlinear Noisy Model of the Microwave FET

In this section we address the difficult problem of deriving a noise description of the FET (or HEMT) operated in a large-signal time-periodic regime. From the theoretical point of view, the starting point here is represented by the well-known noisy equivalent circuit of the dc-biased intrinsic FET, which is shown in Fig. 3 in its most simplified version. This circuit is already in the form of a Norton equivalent, and is thus directly usable within the frame of the general noise analysis approach described in Section II. The spot correlation matrix of the gate and drain noise current sources is [19] (T = device absolute temperature)

$$\boldsymbol{C}_{\mathrm{dc}}(\omega)=\frac{2}{\pi}K_B T d\omega\begin{bmatrix}\dfrac{\omega^2 C_g^2}{g_m}R & -j\omega C_g\sqrt{PR}\,C\\ j\omega C_g\sqrt{PR}\,C & g_m P\end{bmatrix} \tag{16}$$

where the gate and drain noise parameters R and P and the correlation coefficient C are related to the physical noise sources acting in the channel and are thus functions of the device structure and of the bias point. R and P will be referred to as the foundry factors in the following.

In a mixer the FET is not only dc biased, but also pumped by the local oscillator. We accomplish the transition from the static to the dynamic case by a quasi-static assumption, that is, by treating the LO-driven periodic steady state as a time-dependent bias point. Note that this is conceptually similar to using the dc characteristics as instantaneous voltage–current relationships at microwave frequencies, which is a common practice in nonlinear circuit simulation. Under this assumption, we obtain the correlation matrix in dynamic conditions by taking the static correlation matrix (16), and formally replacing the bias point $\boldsymbol{X}_0$ with the periodic steady-state $\boldsymbol{x}_{ss}(t)$ in the expressions of all bias-dependent quantities (i.e., C_g, g_m, R, P, C).

Let us now rewrite (4) for the gate and drain noise current sources of a generic FET in the form

$$\begin{aligned} i_g(t)&=h_g(t)\,i_{g\,\mathrm{dc}}(t,\boldsymbol{X}_0)\\ i_d(t)&=h_d(t)\,i_{d\,\mathrm{dc}}(t,\boldsymbol{X}_0).\end{aligned} \tag{17}$$

If we square the two sides of (17) and take the statistical mean, and remember that h_g and h_d are deterministic functions, from (16) we obtain

$$\begin{aligned} h_g(t)&=\frac{C_g[x_{ss}(t)]}{C_g(\boldsymbol{X}_0)}\cdot\left\{\frac{g_m(\boldsymbol{X}_0)}{g_m[x_{ss}(t)]}\cdot\frac{R[x_{ss}(t)]}{R(\boldsymbol{X}_0)}\right\}^{1/2}\\ h_d(t)&=\left\{\frac{g_m[x_{ss}(t)]}{g_m(\boldsymbol{X}_0)}\cdot\frac{P[x_{ss}(t)]}{P(\boldsymbol{X}_0)}\right\}^{1/2}\end{aligned} \tag{18}$$

In this way the modulating functions required by the general analysis of Section II may be directly computed once the steady-state $\boldsymbol{x}_{ss}(t)$ has been found.

From a practical point of view, the most difficult aspect of the entire procedure is to establish the numerical values of the foundry factors and of the correlation coefficient as well as their functional dependence on the bias point. Theoretical calculations have been carried out by several authors (e.g., [15] and [22]), but the related software is usually not available. Also, the results presented in different papers are sometimes conflicting, so that some kind of experimental support seems to be necessary. We thus need a reliable method for extracting the required data from the usually available noise information, represented by the classic four spot noise parameters. The latter are defined by the well-known expression of the noise figure:

$$F=F_{\min}+\frac{R_N}{G_S}\left[(G_S-G_0)^2+(B_S-B_0)^2\right] \tag{19}$$

where

F = device noise figure at a fixed bias point,
$F_{\min}$ = minimum noise figure,
R_N = noise resistance,
G_S = source conductance,
B_S = source susceptance,
G_0 = optimum source conductance,
B_0 = optimum source susceptance.

The noise parameters, $F_{\min}$, R_N, G_0, and B_0, are obviously frequency- and bias-dependent.

Let us now introduce the admittance matrix $\boldsymbol{y}$ of the intrinsic FET. Making use of conventional noise analysis (e.g., [20]), the spot correlation matrix of the gate and drain noise current sources may be expressed as

$$\boldsymbol{C}_{\mathrm{dc}}(\omega)=\frac{2}{\pi}K_B T d\omega\begin{bmatrix}G_N+|Y_N|^2R_N & y_{21}^*Y_N R_N\\ y_{21}Y_N^*R_N & |y_{21}|^2R_N\end{bmatrix} \tag{20}$$

where

$$\begin{aligned} G_N&=G_0(F_{\min}-1)-\frac{(F_{\min}-1)^2}{4R_N}\\ Y_N&=y_{11}+G_0+jB_0-\frac{F_{\min}-1}{2R_N}.\end{aligned} \tag{21}$$

Note that the inverse relationships of (20) and (21) are also explicitly available [20].

Of course, (20) and (16) must coincide, so that the foundry factors must be related to the admittance and

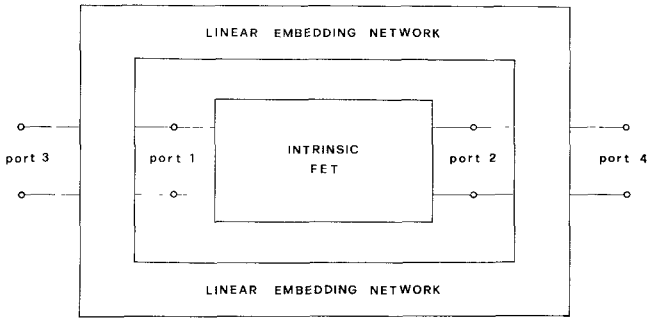

Fig. 4. Schematic representation of an extrinsic FET device.

noise parameters by the equations

$$P = |y_{21}|^2 \frac{R_N}{g_m}$$

$$R = \frac{g_m\left(G_N + |Y_N|^2 R_N\right)}{\omega^2 C_g^2}$$

$$jC = \frac{y_{21}}{|y_{21}|} Y_N^* \left(\frac{R_N}{G_N + |Y_N|^2 R_N} \right)^{1/2}. \tag{22}$$

Equations (22) cannot be directly used to extract the foundry factors from measured quantities, since they make use of the noise parameters of the intrinsic FET, which are not directly measurable. This difficulty may be overcome by making use of the noise de-embedding procedure described below. As shown in Fig. 4, the extrinsic FET can be represented as the intrinsic device embedded in a linear 4-port, which is used to model the relevant parasitic effects. This network is known from well-established linear modeling approaches.

If we denote by $\boldsymbol{Y}$ the admittance matrix of the embedding network, we can partition $\boldsymbol{Y}$ into 2×2 submatrices as follows:

$$\boldsymbol{Y} = \begin{bmatrix} \boldsymbol{Y}_{it} & \boldsymbol{Y}_{ie} \\ \boldsymbol{Y}_{et} & \boldsymbol{Y}_{ee} \end{bmatrix} \tag{23}$$

where the subscripts i and e stand for "intrinsic" and "extrinsic," respectively (see Fig. 4). Making use of the linear noise analysis method discussed in [20], we can relate the noise correlation matrix of the extrinsic FET, namely $\boldsymbol{C}_e(\omega)$, to that of the intrinsic device by the equation (see [20, eqs. (18) and (19)])

$$\boldsymbol{C}_e = \boldsymbol{M}\,\mathrm{Re}(\boldsymbol{Y})\boldsymbol{M}^* + \boldsymbol{M}_t \boldsymbol{C}_{\mathrm{dc}} \boldsymbol{M}_t^* \tag{24}$$

where

$$\boldsymbol{M}_t = -\boldsymbol{Y}_{et}\left(\boldsymbol{Y}_{it} + \boldsymbol{y}\right)^{-1}$$

$$\boldsymbol{M} = [\boldsymbol{M}_t | \boldsymbol{I}_2] \tag{25}$$

($\boldsymbol{I}_2$ = identity matrix of order 2). Equation (24) takes into account the fact that the embedding network is reciprocal. From (24) through (25) and (23) we obtain

$$\boldsymbol{C}_{\mathrm{dc}} = \boldsymbol{N}_t\left[\boldsymbol{C}_e - \mathrm{Re}(\boldsymbol{Y}_{ee})\right]\boldsymbol{N}_t^* - \boldsymbol{N}_t\,\mathrm{Re}(\boldsymbol{Y}_{et}) - \mathrm{Re}(\boldsymbol{Y}_{te})\boldsymbol{N}_t^* - \mathrm{Re}(\boldsymbol{Y}_{tt}) \tag{26}$$

where $\boldsymbol{N}_t = \boldsymbol{M}_t^{-1}$.

The overall identification procedure can thus be summarized as follows: i) the measured noise and admittance parameters of the extrinsic FET are used to compute $\boldsymbol{C}_e$ by equations similar to (20) and (21); ii) an equivalent circuit of the extrinsic FET is found and the admittance matrix of the embedding network is derived; iii) $\boldsymbol{C}_{\mathrm{dc}}$ is computed by (26), the intrinsic noise parameters are extracted from (20) and (21), and the foundry factors are obtained by means of (22).

In practice, the combination of the measurement errors with the de-embedding process (the latter requiring the intervention of the device parasitics) can produce some uncertainties in the estimated intrinsic noise parameters. Thus the above procedure is best used in a least-squares sense, for instance to approximate the noise data measured over a frequency band at a fixed bias point. Under this respect, the use of a simple theoretical model through a parameter fit to measured data is very convenient, because it effectively helps to smooth out errors and inconsistencies of any kind.

A further important point is that the measured noise parameters are usually affected by a noise contribution arising from ohmic losses in the device measurement setup. Following Gupta [23], this contribution is accounted for by means of an equivalent noise conductance G_c connected in parallel at the device input (i.e., at port 3 in Fig. 4), which is treated as an additional free parameter in the fitting process.

As an example of an application, we consider an Avantek AT 8251 FET biased at $V_{ds} = 3$ V, $I_{ds} = 20$ mA. Fig. 5 shows the best fit to the measured behavior of the minimum noise figure $F_{\min}$ in the 1–10 GHz band, with and without an input noise conductance. The sets of parameters corresponding to the two computed curves are

$$\begin{aligned} G_c &= 0 \\ P &= 2.01 \\ R &= 0.40 \\ C &= 0.71 \end{aligned} \tag{27}$$

and

$$\begin{aligned} G_c &= 1/2400\ \Omega \\ P &= 2.05 \\ R &= 0.19 \\ C &= 0.88. \end{aligned} \tag{28}$$

The values (28) give an excellent fit between measured and computed noise parameters, the maximum error on $F_{\min}$ (e.g.) being of the order of 0.1 dB. Also, the estimates of the foundry factors and of the correlation coefficients are

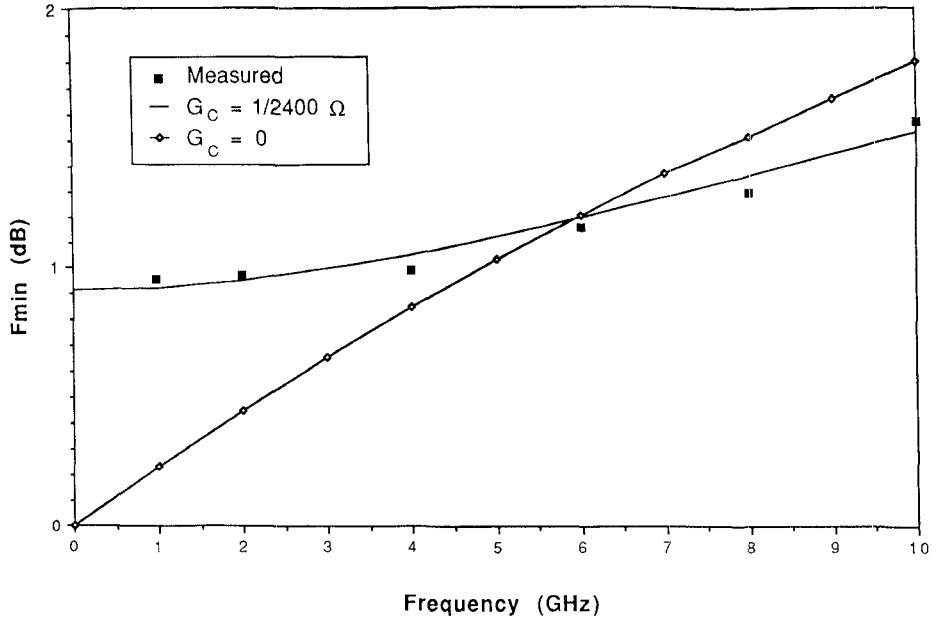

Fig. 5. Minimum noise figure of the AT 8251 at $V_{ds} = 3$V, $I_{ds} = 20$ mA.

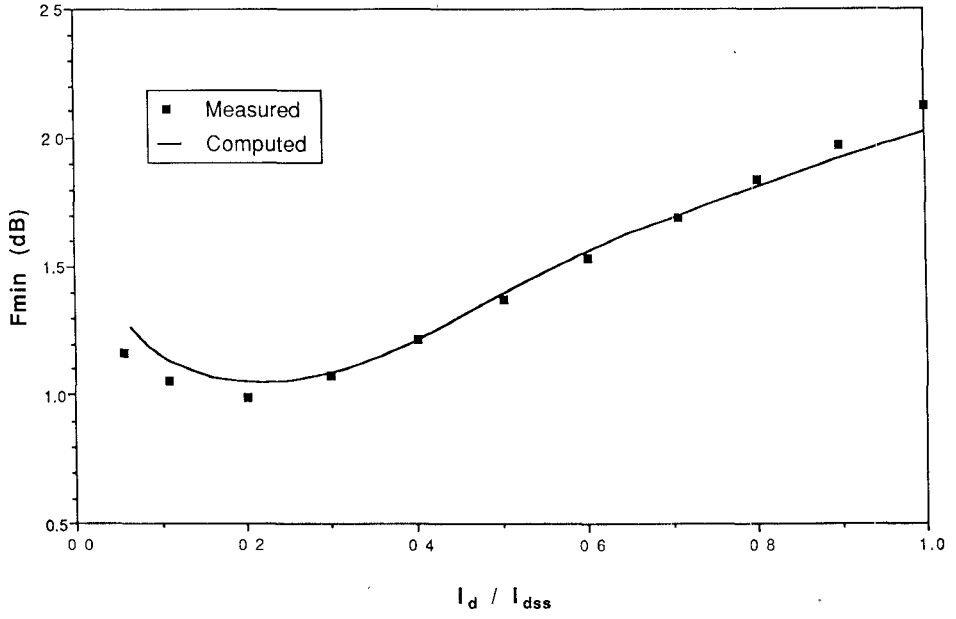

Fig. 6 Minimum noise figure of the AT 8251 at $V_{ds} = 3$V, $f = 4$ GHz.

well within the typical ranges [15]. On the other hand, a comparison between the two computed curves clearly shows that the circuit noise conductance G_c provides the only means of accurately modeling the low-frequency behavior of F_{min}. Note that because of its numerical value, G_c has no effect on any aspects of the FET performance other than noise, and thus cannot be detected by scattering-matrix calculations.

In order to find the dependence of the foundry factors on the bias point, the whole procedure can be repeated for several bias settings of the active device. A check of the accuracy of the overall noise model derived in this way is given in Fig. 6. Here, the computed minimum noise figure of the AT8251 at $V_{ds} = 3$ V and $f = 4$ GHz is plotted against the drain current and compared with the measured values available from the data sheet. Once again the fit is excellent, with maximum errors of the order of 0.1 dB.

IV. Final Considerations and Results

As an example of application, let us consider a FET gate mixer whose schematic description in terms of a lumped-element equivalent circuit is given in Fig. 7. This circuit was designed for an RF bandwidth ranging from 8.1 to 9.1 GHz with an 8 GHz local oscillator. The design was

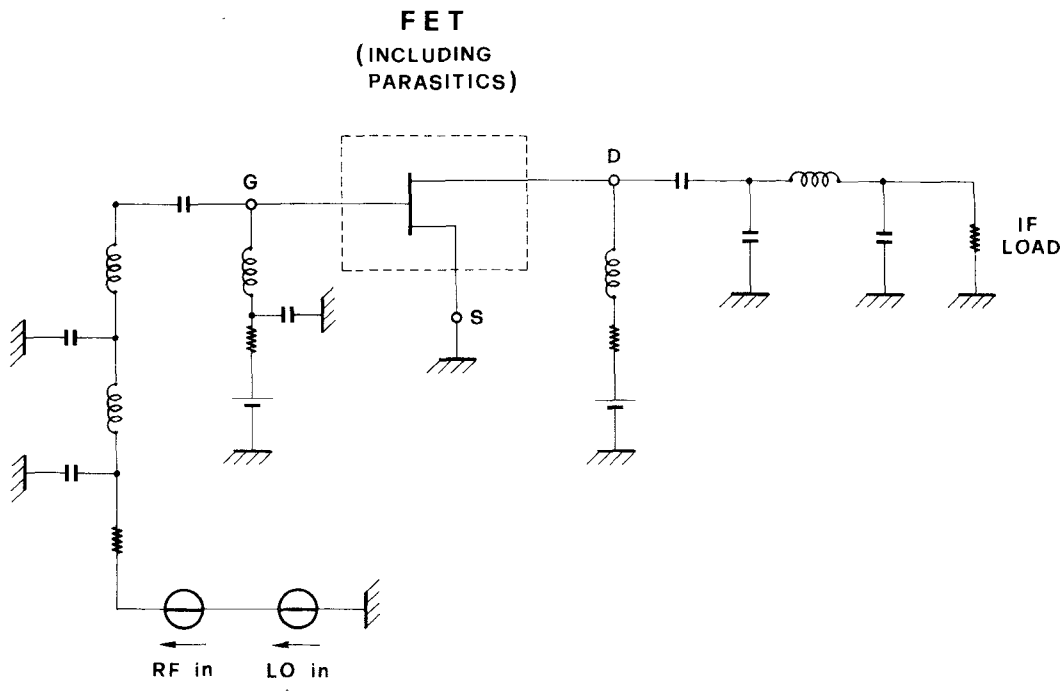

Fig. 7. Lumped-element equivalent circuit of a single-ended FET gate mixer

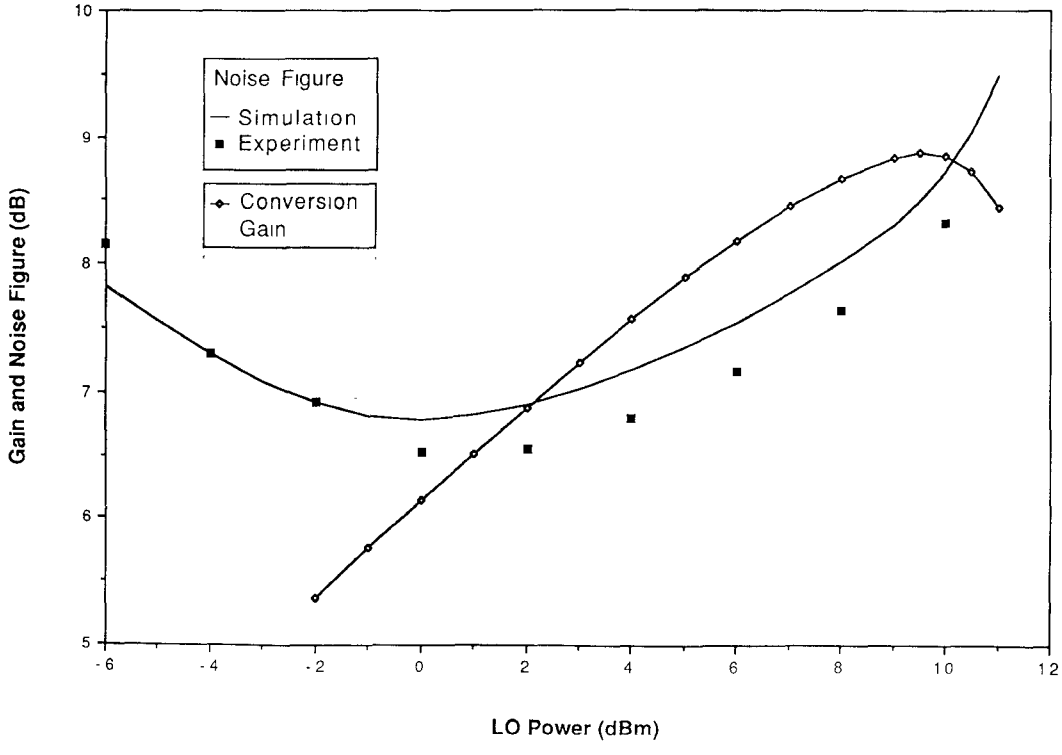

Fig. 8. Gain and noise performance of the FET mixer depicted in Fig 7.

carried out by a general-purpose harmonic-balance simulator with optimization capabilities [13], and the mixer was realized in hybrid form using an AT 8251 device. A nonlinear time-domain equivalent circuit of the active device was derived from dc and scattering-matrix measurements by a procedure similar to that described in [24]. For optimum noise performance the FET was biased very close to pinch-off ($V_{gs} = -1.4$ V, $V_{ds} = 3$ V).

The behavior of this mixer is illustrated in Fig. 8 in the case of an 800 MHz IF. The black square dots show the dependence of the measured noise figure on local oscillator power with a 50 Ω source and load. The noise figure has a relatively flat minimum at power levels below 3 dBm, with an absolute minimum value of 6.5 dB around 0 dBm. The computed results also shown in the figure are in very good agreement with the measured ones. The error on the mini-

mum noise figure is about 0.3 dB, and the two curves appear to be shifted by approximately 0.5 dB on the average.

For comparison, the mixer conversion gain is also plotted in the same figure as a function of LO power. The observed shift between the gain maximum and the noise figure minimum is due to the bias dependence of the foundry factors. The device is biased near pinch-off, which means close to a minimum of the drain noise power [15], and the gate voltage swing in maximum-gain conditions is large. Decreasing the LO power thus results in a reduction of the internally generated noise and of the noise figure as well. This trend lasts until the quick drop of the conversion gain causes the noise figure to rise again. Thus the noise figure minimum is considerably shifted backwards. This result is consistent with several experimental observations (e.g., [4], [8]–[10]).

To carry out the computations a program was written having the structure of a set of subroutines which work in conjunction with a general-purpose harmonic-balance simulator [13]. The FET models have been enhanced to include the noise sources and to accept the measured noise parameters, besides the conventional equivalent-circuit information, as input data. The analysis of the local oscillator regime and the various steps of the noise analysis are then carried out automatically. The program accepts an arbitrary user-defined linear subnetwork topology. For the single-ended FET gate mixer the whole noise analysis takes about one fourth of the CPU time required by the harmonic-balance analysis of the local oscillator regime. Thus once the necessary software has been developed, noise information becomes available at little additional cost beyond that of a conventional mixer analysis.

A completely general-purpose program for the noise analysis of nonlinear microwave circuits should include a $1/f$ noise source. This may be significant for mixers with a low IF (less than a few MHz), and is certainly necessary to describe the near-carrier noise in oscillators.

In principle the inclusion of such a source is straightforward, since it can be treated in exactly the same way as any other one. Specifically, this source may be represented as an equivalent current source to be connected in parallel to i_g at the intrinsic FET input (Fig. 3), which leads to the appearance of an additive term in the 1–1 element of the correlation matrix (16). Since empirical descriptions of the bias dependence of the $1/f$ source are available in the literature (e.g., [25]), the modulating function for this source can easily be derived, and the analysis method of Section II becomes directly applicable.

In practice, there is experimental evidence reported in the literature that the sideband correlation properties of the $1/f$ source are somewhat anomalous due to the complexity of the related physical mechanisms [25]. The important point here is that our numerical approach allows empirical corrections of the sideband correlation coefficients to be introduced, if necessary, without any difficulty, since the correlation matrix (7) is explicitly made available by the program at an intermediate step of the computational procedure.

In conclusion we can foresee that in the near future the capabilities of present-day harmonic-balance simulators will be complemented by facilities for noise calculation in general nonlinear microwave circuits.

References

[1] D. N. Held and A. R. Kerr, "Conversion loss and noise of microwave and millimeter-wave mixers: Part 1—Theory," *IEEE Trans. Microwave Theory Tech.*, vol. MTT-26, pp. 49–55, Feb. 1978.

[2] A. R. Kerr, "Noise and loss in balanced and subharmonically pumped mixers: Part 1—Theory," *IEEE Trans. Microwave Theory Tech.*, vol. MTT-27, pp. 938–943, Dec. 1979.

[3] M. T. Faber and W. K. Gwarek, "Nonlinear-linear analysis of microwave mixers with any number of diodes," *IEEE Trans. Microwave Theory Tech.*, vol. MTT-28, pp. 1174–1181, Nov. 1980.

[4] S. A. Maas, "Theory and analysis of GaAs MESFET mixers," *IEEE Trans. Microwave Theory Tech.*, vol. MTT-32, pp. 1402–1406, Oct. 1984.

[5] J. Dreifuss, A. Madjar, and A Bar-Lev, "A novel method for the analysis of microwave two-port active mixers," *IEEE Trans. Microwave Theory Tech.*, vol. MTT-33, pp. 1241–1244, Nov. 1985.

[6] *MICROWAVE HARMONICA User Manual*, Compact Software Inc., 483 McLean Blvd., Paterson, NJ, 1988.

[7] *LIBRA User Manual*, EEsof Inc., 5795 Lindero Canyon Rd., Westlake Village, CA, 1988.

[8] G. K. Tie and C. S. Aitchison, "Noise figure and associated conversion gain of a microwave MESFET gate mixer," in *Proc. 13th European Microwave Conf.* (Nürnberg), Sept. 1983, pp. 579–584.

[9] J. Dreifuss, A. Madjar, and A. Bar-Lev, "A novel method for calculating the noise figure of microwave MESFET mixers," in *Proc. 17th European Microwave Conf.* (Rome), Sept. 1987, pp. 466–471.

[10] S. A. Maas, *Microwave Mixers*. Dedham MA: Artech House, 1986.

[11] S. A. Maas, *Nonlinear Microwave Circuits*. Norwood, MA: Artech House, 1988.

[12] V. Rizzoli and A. Neri, "State of the art and present trends in nonlinear microwave CAD techniques," *IEEE Trans. Microwave Theory Tech.*, vol. 36, pp. 343–365, Feb. 1988.

[13] V. Rizzoli *et al.*, "General-purpose harmonic-balance analysis of nonlinear microwave circuits under multitone excitation," *IEEE Trans. Microwave Theory Tech.*, vol 36, pp. 1650–1660, Dec. 1988.

[14] C. Rumelhard, "Large-signal models of MESFET and HEMT," presented at the Workshop on Non Linear CAD Tools for Microwave and Millimetre Wave (Integrated) Circuit Analysis, Stockholm, Sept. 16, 1988.

[15] A. Cappy, "Noise modeling and measurement techniques," *IEEE Trans. Microwave Theory Tech.*, vol. 36, pp. 1–10, Jan. 1988.

[16] G. Begemann and A. Jacob, "Conversion gain of MESFET drain mixers," *Electron. Lett.*, vol. 15, no. 18, pp. 567–568, Aug 1979.

[17] T. Ohta *et al.*, "Very small and light *Ku*-band low noise converter with low noise FET mixer," in *Proc. 18th European Microwave Conf.* (Stockholm), Sept. 1988, pp. 451–456.

[18] M. S. Nakhla and J Vlach, "A piecewise harmonic-balance technique for determination of periodic response of nonlinear systems," *IEEE Trans. Circuits Syst.*, vol. CAS-23, pp. 85–91, Feb. 1976.

[19] H. Statz, H. A. Haus, and R. A. Pucel, "Noise characteristics of gallium arsenide field-effect transistors," *IEEE Trans. Electron Devices*, vol. ED-21, pp. 549–562, Sept. 1974.

[20] V. Rizzoli and A. Lipparini, "Computer-aided noise analysis of linear multiport networks of arbitrary topology," *IEEE Trans. Microwave Theory Tech.*, vol. MTT-33, pp 1507–1512, Dec. 1985.

[21] V. Rizzoli, C. Cecchetti, and A. Lipparini, "Frequency conversion in general nonlinear multiport devices," in *1986 IEEE MTT-S Int. Microwave Symp. Dig.* (Baltimore), June 1986, pp. 483–486.

[22] C. R. Brewitt-Taylor *et al.*, "Noise figure of MESFETS," *Proc. Inst. Elec. Eng*, pt. I, vol. 127, pp. 1–9, Feb. 1980.

[23] M. S. Gupta *et al.*, "Microwave noise characterization of GaAs MESFET's: Evaluation by on-wafer low-frequency output noise

current measurements," *IEEE Trans. Microwave Theory Tech.*, vol. MTT-35, pp. 1208–1218, Dec. 1987.

[24] A. K. Jastrzebski, "Non-linear MESFET modelling," in *Proc. 17th European Microwave Conf.* (Rome), Sept. 1987, pp. 599–604.

[25] H. J. Siweris and B. Schiek, "A GaAs FET oscillator noise model with a periodically driven noise source," in *Proc. 16th European Microwave Conf.* (Dublin), Sept. 1986, pp. 681–686.

Vittorio Rizzoli (M'79) was born in Bologna, Italy, in 1949. He graduated from the School of Engineering, University of Bologna, in July 1971.

From 1971 to 1973, he was with the Centro Onde Millimetriche of Fondazione Ugo Bordoni, Pontecchio Marconi, Italy, where he was involved in research on millimeter-waveguide communication systems. In 1973, he was with the Hewlett-Packard Company, Palo Alto, CA, working in the areas of MIC and microwave power devices. From 1974 to 1979, he was an Associate Professor at the University of Bologna, teaching a course on microwave integrated circuits. In 1980, he joined the University of Bologna as a Full Professor of Electromagnetic Fields and Circuits. His current research interests are in the fields of MIC and MMIC, with special emphasis on nonlinear circuits. He is also heading a research project aimed at the development of vectorized software for microwave circuit design applications.

Franco Mastri was born in Forlì, Italy, in 1957. He graduated in electronic engineering from the University of Bologna in 1985.

In 1987 and 1988 he obtained research grants issued by Fondazione G. Marconi, Italy, and Selenia S.p.A., Rome, Italy, to carry out a study on the application of nonlinear CAD techniques in MIC and MMIC design. His research activity is mainly devoted to nonlinear microwave device modeling and characterization and to the development of software tools for microwave circuit design.

Claudio Cecchetti was born in Forlì, Italy, in 1957. He graduated in electronic engineering from the University of Bologna in October 1983.

In 1984 and early 1985 he obtained a research grant issued by Fondazione G. Marconi, Pontecchio Marconi, Italy, to develop user-friendly interactive software for linear microwave circuit CAD. In 1985, he joined Fondazione U. Bordoni, Rome, Italy, where he is currently involved in research on nonlinear microwave circuit design. His main field of interest is the development of vectorized software for MIC and MMIC design applications.